

Spectroscopic and Electrochemical Characterization of CD4 Binding Site of HIV-1 Exterior Envelope gp120

Natalia Cernei^{1,2}, Zbynek Heger¹, Pavel Kopel^{1,2}, Vedran Milosavljevic¹, Marketa Kominkova¹, Amitava Moulick², Ondrej Zitka^{1,2}, Libuse Trnkova², Vojtech Adam^{1,2}, Rene Kizek^{1,2*}

¹ Department of Chemistry and Biochemistry, Faculty of Agronomy, Mendel University in Brno, Zemedelska 1, CZ-613 00 Brno, Czech Republic, European Union

² Central European Institute of Technology, Brno University of Technology, Technicka 3058/10, CZ-616 00 Brno, Czech Republic, European Union

*E-mail: kizek@sci.muni.cz

Received: 18 January 2014 / Accepted: 17 March 2014 / Published: 14 April 2014

Glycoprotein 120 (gp120) is essential biomolecule for HIV-1 entry into cells as it plays a vital role in attachment to specific cell surface receptors. Exterior envelope glycoprotein 120 contains conservative CD4 binding site in its structure that may be one of target molecules for development of HIV therapeutic agents, able to inhibit the viral entry steps into the host cells. The present study describes the solid-phase, Fmoc-based synthesis of CD4 binding site (SSGGD PEIVMH), and its subsequent spectroscopic characterization, with determined purity over 90 %. Moreover; electrochemical analyses were carried out to optimize the conditions for peptide determination. Using the optimized conditions as Britton-Robinson buffer with pH 8 and 3% addition of acetonitrile (v/v) as a mobile phase, potential 1100 mV, limit of detection of 0.04 $\mu\text{g}\cdot\text{mL}^{-1}$ and limit of quantification of 0.1 $\mu\text{g}\cdot\text{mL}^{-1}$ were estimated.

Keywords: CD4 binding loop; gp120; Human immunodeficiency virus-1; Peptide synthesis

1. INTRODUCTION

Human immunodeficiency virus type 1 (HIV-1) is characterized by extensive genetic variability, as a consequence of high replication and mutation rates and frequent recombination [1,2]. HIV destroys the human immune system and causes lethal diseases such as acquired immune deficiency syndrome (AIDS) [3], one of the most devastating disease, attacking humanity today, affecting 65 million people with 11 000 new cases per day [4].

HIV-1 entry depends on the sequential interaction with the CD4 receptors on the CD4⁺ T cells and the members of the chemokine receptor family [5]. The entry of HIV-1 into cell is mainly mediated by the viral envelope glycoproteins [6], which are synthesized as an ~850- amino acid

precursor. After trimerization and posttranslational modification by carbohydrate, 160-kDa glycoprotein (gp160) is formed. Proteolysis of gp160, processed in the Golgi apparatus, provides a creation of gp120 exterior envelope glycoprotein containing relatively conserved CD4 binding site and gp41 *trans*-membrane envelope glycoprotein [7-9]. In the mature HIV-1 envelope glycoprotein trimer, the three gp120 subunits are noncovalently bound to three membrane-anchored gp41 subunits [10], as it can be seen in Fig. 1.

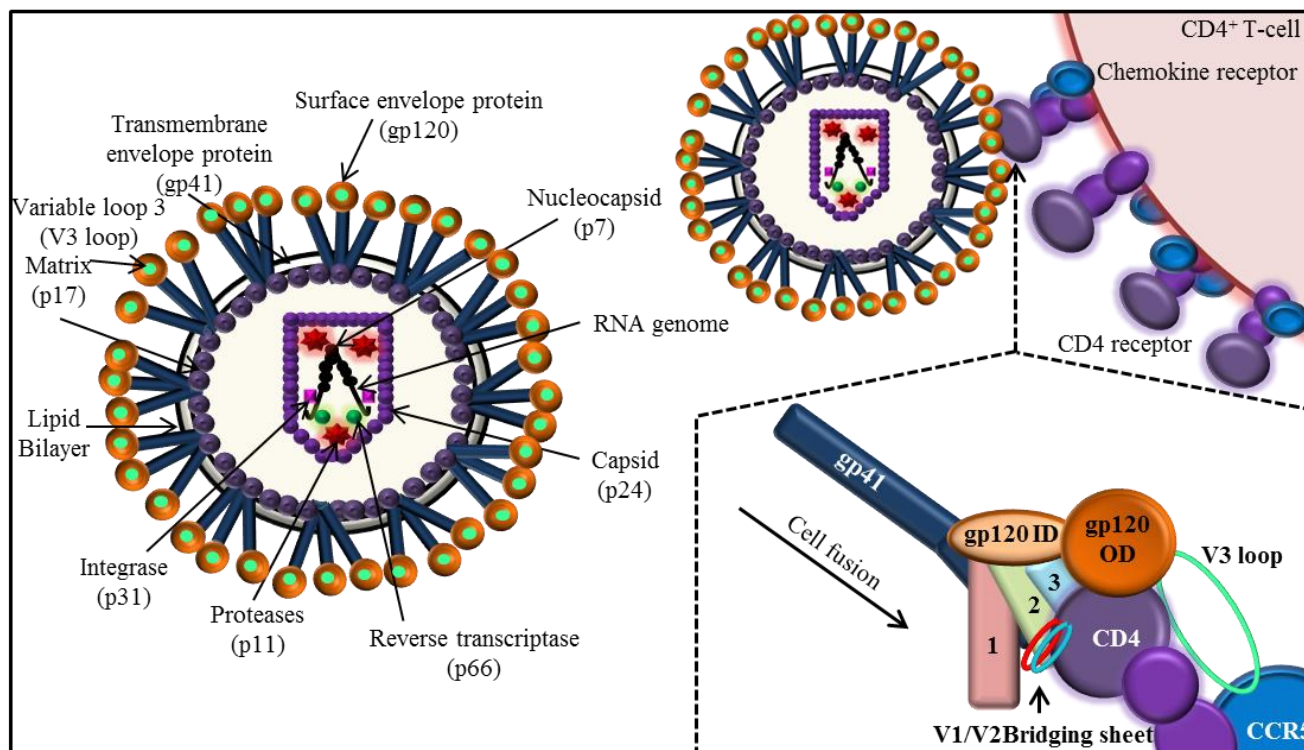


Figure 1. Overall scheme of HIV-1 virion with the expression of interaction between HIV-1 envelope glycoproteins with CD4 receptor binding site. One of the subunit of gp41 is depicted. Binding with CD4 results in the apposition of layer 1 and layer 2, the formation of the bridging sheet and the projection of the V3 loop away from the gp120 core towards coreceptor. This rearrangement of gp120 allows the gp41 ectodomain to undergo additional conformational changes, necessary for HIV-1 entry. The **gp120 OD** stays for outer domain of glycoprotein 120, **gp120 ID** stays for inner domain of glycoprotein 120, **1; 2; 3** stays for loops that form three topological layers and **CCR5** stays for coreceptor (chemokine receptor).

For entry of HIV-1 into a host cell, the gp120 subunit associates with the CD4 receptor and the CCR5 coreceptor, and this induces series of conformational changes culminating in virus and host cell membrane fusion. Most primary HIV-1 strains use the chemokine receptor CCR5 as coreceptor in conjunction with CD4 for virus entry. However, some strains has evolved to use related receptors [11]. Binding of gp120 to CD4 causes conformational changes observable in variable loop regions V1/V2 and V3, causing the V3 loop to evaginate, thus becoming exposed to the co-receptors [12], which is shown in Fig. 1. The precise mechanisms of interaction between V1/V2, V3 and chemokine receptors are not well understood [13]. The final step of viral entry, fusion of the viral

components with target membrane, is achieved by gp 41 [14,15]. After binding of gp120 to CD4 and coreceptors, conformational changes occur, leading to gp41 unfolding and the hydrophobic fusion peptide sequence extends towards the host cell membrane [16]. The insertion of the peptide leads to fold into a hairpin-like structure, believed to be responsible for the fusion of the HIV to the host cell [17].

Due to the nature of fusion, there are several possible targets for the development of drugs with synergistic effects on inhibition of viral entry steps, at which the interference can be attempted. Generally, these targets may affect viral entry by the inhibition of CD4 binding due to a blocking of conservative CD4 binding site of gp120. Hence, glycoprotein cannot interact with receptors and coreceptors and process of conformational changes, whereas the triggering the fusion is stopped.

Therefore, the aim of this study was a synthesis of CD4 binding site and its subsequent spectroscopic characterization. Moreover, electrochemical measurements were carried out to optimize the conditions for analyses serving for rapid and accurate monitoring of various peptide-peptide interactions helpful for development of new potential peptides with antiviral or other effects.

2. EXPERIMENTAL PART

2.1. Chemicals and pH measurement

Working solutions like buffers and standard solutions were prepared daily by diluting the stock solutions. Standards and other chemicals were purchased from Sigma-Aldrich (St. Louis, MO, USA) meets the specification of American Chemical Society (ACS), unless noted otherwise. Methyl cellosolve as well as tin chloride were purchased from Ingos (Prague, Czech Republic). Deionised water underwent demineralization by reverse osmosis using the instruments Aqua Osmotic 02 (Aqua Osmotic, Tisnov, Czech Republic) and then it was subsequently purified using Millipore RG (Millipore Corp., USA, 18 M Ω) – MiliQ water.

2.2. Synthesis of CD4 binding loop of gp120

Peptide (SSGGD PEIVMH) with molecular mass of 1908 was prepared using Liberty Blue peptide synthesizer (CEM, Matthews, NC, USA) by standard f-moc solid-phase peptide synthesis. Fourfold excess of f-moc amino acid was used with respect to the resin. As the first step 167 mg of rink amide was swelled in 10 mL of N,N-dimethylformamide (DMF) for 1 hour. For preparation of activator 9.48 g of N,N,N',N'-tetramethyl-O-(1H-benzotriazol-1-yl)uronium hexafluorophosphate (HBTU) was dissolved in 50 mL of DMF. As an activator base 17.4 mL of N,N-diisopropylethylamine (DIEA) was mixed with 32.6 mL of DMF. Deblocking of f-moc protecting groups was carried out using 20% piperidine (v/v) in 80% DMF (v/v). For each amino acid, microwave deprotection was performed for 2 minutes at 80 °C and 15 PSI. For each amino acid, microwave coupling was carried out for 5 minutes at 89 °C, 15 PSI and 150 W (except of coupling of histidine, where 50 °C was applied). Entire synthesis was carried out for 1 hour and synthesized peptides, attached with rink

amide, were taken out from reaction vessel, mixed with 10 mL of dichloromethane and replaced into a vacuum cleaner tube used for removal of the solvent and other undesired chemicals. The cleavage of groups protecting the side chains was performed by treatment of peptide resin with 95% trifluoroacetic acid (TFA) (v/v), 2.5% H₂O (v/v), and 2.5% triisopropylsilane (v/v) for 30 minutes in Discovery microwave (CEM, Matthews, NC, USA) at 38 °C. Further, into solution of peptide with cleavage cocktail, diethylether used for peptide precipitation was added. Resulting solution was centrifuged (6000 rpm, 4 min, 0 °C) and the supernatant was discarded. Peptide synthesized in this way was prepared for subsequent experiments.

2.3 UV/Vis Spectrophotometry

Absorption spectra were recorded within the range from 220 to 700 nm on spectrophotometer SPECORD 210 (Analytik Jena, Jena, Germany) using quartz cuvettes (1 cm, Hellma, Essex, UK). Cuvette space was tempered by a thermostat Julabo (Labortechnik, Wasserburg, Germany) to temperature 25 °C. After a measurement, cuvettes were rinsed with deionised water and dried with nitrogen.

2.4 Acidic hydrolysis

1 mg of peptide was mixed with 0.5 mL of 6 M HCl and solution was subsequently subjected to digestion in a microwave reactor Anton Paar (Anton Paar GmbH, Graz, Austria) using the following conditions: power 80, ramp 15 minutes, hold 90 minutes, maximum 120 °C and maximum pressure 25 bar. Further, the hydrolysed sample was diluted with the dilution buffer composed of 5 mL.L⁻¹ of thiodiglycol, 14 g.L⁻¹ of citric acid, 11.5 g.mL⁻¹ of sodium chloride and centrifuged using Microcentrifuge 5417R (Eppendorf AG, Hamburg, Germany) using 25,000 g at 4 °C for 10 min.

2.5 Ion-exchange chromatography

For identification of peptide and its amino acid composition, the ion-exchange liquid chromatography with post column derivatization by ninhydrin and the absorbance detector in the VIS range set to 440 nm was employed. Glass column, tempered to 60 °C with inner diameter of 3.7 mm and 350 mm length, was filled manually with strong cation exchanger in sodium cycle LG ANB with approximately 12 µm particles and 8% porosity. Experimental conditions were applied according to our preliminary study [18].

2.6 Matrix-assisted laser desorption/ionization-time of flight mass spectrometry

Confirmation of successful peptide synthesis was performed on a MALDI-TOF/TOF mass spectrometer Bruker ultrafleXtreme (Bruker Daltonik GmbH, Germany) equipped with a laser operating at wavelength of 355 nm with an accelerating voltage of 25 kV, cooled with nitrogen and

with a maximum energy of 43.2 μJ . The matrix used in the MALDI method was a 2,5-dihydroxybenzoic acid (Sigma-Aldrich). The saturated matrix solution was prepared in 50% methanol (v/v) and 0.1% trifluoroacetic acid (v/v). Mixture was vortexed and ultrasonicated using Bandelin 152 Sonorex Digital 10P ultrasonic bath (Bandelin electronic GmbH, Germany) for 2 minutes at 50 % intensity at room temperature. A dried-droplet method was used for sample preparation. Briefly, the sample solution was mixed with matrix solution in volume ratio 1:1. After the obtaining a homogeneous solution, 2 μL of mixture was applied on the target plate and dried under atmospheric pressure at room temperature. The mass spectra were acquired by averaging 2000 subspectra from a total of 2000 shots of the laser. Laser power was set 5-10 % above the threshold.

2.7 Flow injection analysis with electrochemical detection

Flow injection analysis with electrochemical detection (FIA-ED) system consisted of two chromatographic pumps Model 582 ESA (ESA Inc., Chelmsford, USA) with working range 0.001 - 9.999 $\text{mL}\cdot\text{min}^{-1}$ and CoulArray electrochemical detector (Model 5600A, ESA, USA). Detector consisted of flow analytical chamber (Model 6210, ESA, USA). The chamber contains four analytical cells. One analytical cell contains two referent (hydrogen-palladium), and two counter electrodes and one porous graphite working electrode. Electrochemical detector is situated in control module, which is thermostated. Sample (20 μL) was injected by manual valve (Rheodyne, Oak Harbor, WA, USA). Flow rate of mobile phase was 1 $\text{mL}\cdot\text{min}^{-1}$.

2.8 Descriptive statistics

Mathematical analysis of the data and their graphical interpretation were realized by Microsoft Excel®, Microsoft Word® and Microsoft PowerPoint®. Results are expressed as mean \pm standard deviation (S.D.) unless noted otherwise. The detection limits (3 signal/noise, S/N) were calculated according to Long and Winefordner [19], whereas N was expressed as standard deviation of noise determined in the signal domain unless stated otherwise.

3. RESULTS AND DISCUSSION

HIV-1 infection is characterized by rapid and extensive CD4^+ T-cells depletion and immunodeficiency leading to the decreased immune response and to infection facilitating viral persistence, and increased viral loads and transmission rates [20,21]. Based upon this information, CD4 binding site of gp120 may exhibit large potential in the development of therapeutic agents able to block this structure and thus prevent the HIV virion fusion with host cell.

3.1 Synthesis of CD4 binding site-like peptide

In this study, firstly, the synthesis of peptide, comprising Ser-Ser-Gly-Gly-Asp Pro-Glu-Ile-Val-Met-His (SSGGD PEIVMH, calculated mass 1098.13 Da), was carried out. Peptide synthesis was

performed on a solid-phase, employing 9-Fluorenylmethoxycarbonyl (Fmoc) for side chains protection [22]. Resulting peptide imitates the CD4 binding site of exterior envelope glycoprotein 120 of HIV-1 responsible for affinity towards CD4 receptor localized on membrane of CD4⁺ T-cells. Success rate of CD4 binding site peptide synthesis can be seen in Fig. 2A, where record obtained from Liberty blue synthesizer is shown. Two columns for each amino acid and resin, used in synthesis represent the initial absorbance (left column) and absorbance after synthesis (right column). Low values in the right column point at successful synthesis due to a low amount of amino acid remained in reactor (Fig. 2A). This implies that overwhelming majority of amino acid was correctly linked into peptide chain on the resin.

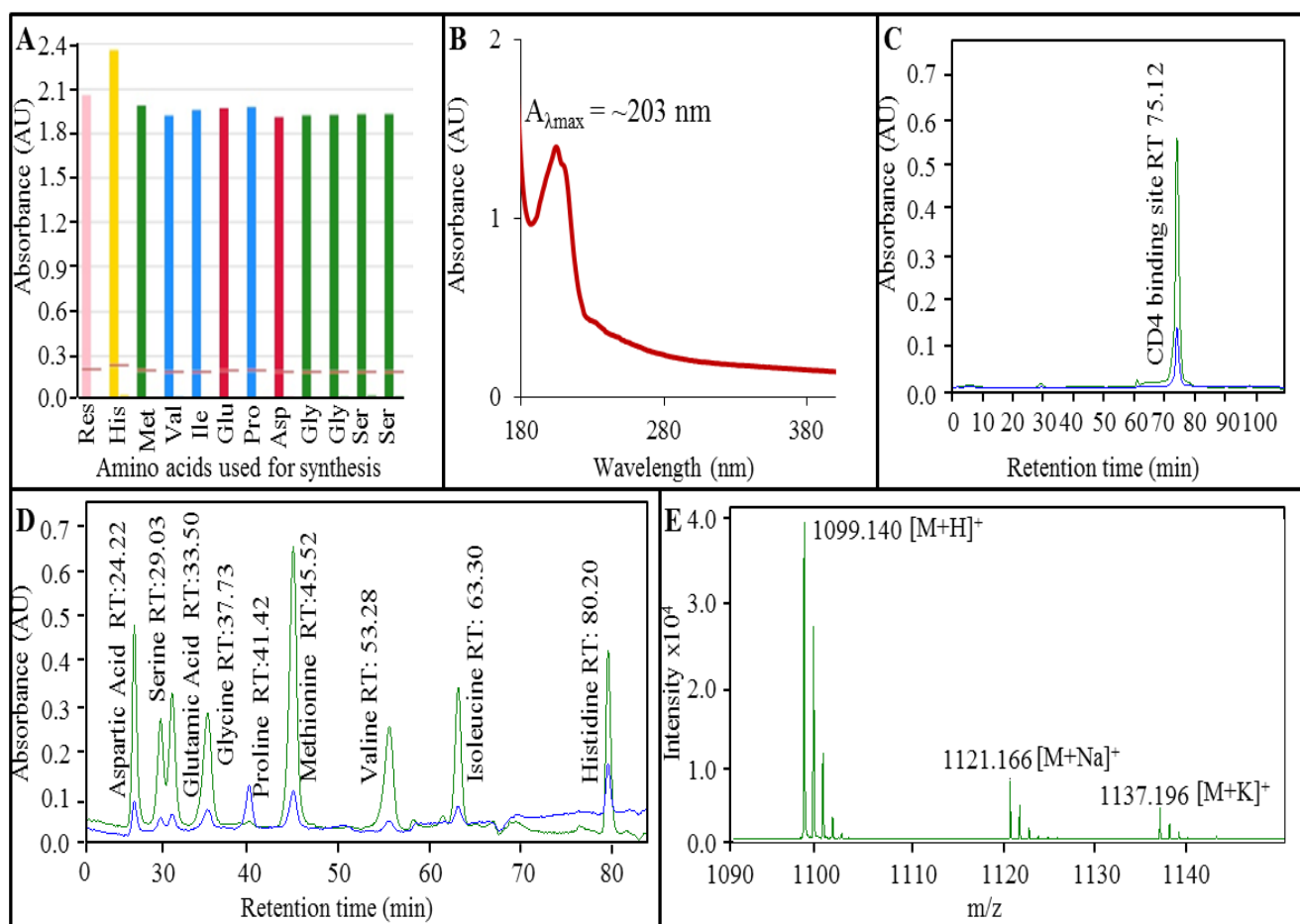


Figure 2. (A) Record obtained from program Liberty Blue, confirming successful synthesis of CD4 binding site (SSGGD PEIVMH), contained in region 366 – 376 of gp120 of HIV-1. (B) Absorption spectra of synthesized CD4 binding site with absorption maximum at 203 nm ($c = 1 \text{ mg.mL}^{-1}$). (C) Typical chromatogram obtained on ion-exchange chromatography (IEC) showing retention time (75.12 min) of CD4 binding site peptide. (D) Expression of amino acid content in CD4 binding site after hydrolysis in microwave reactor MW 3000. (E) MALDI-TOF/TOF mass spectra of CD4 binding site peptide with calculated mass of 1098.13 Da. DHB was used as a matrix. Measurements were carried out in reflector positive mode, with laser power of 70 %. One spectrum is made as an average from 2500 subspectra. **M** stays for molecule of analyte; **H** stays for atom of hydrogen.

3.2 UV/Vis spectrophotometry

To determine the optical properties of synthesized compound, UV/Vis spectrophotometry was employed. As it can be seen in Fig. 2B, CD4 binding site-like peptide shows its absorption maxima at ~203 nm. The absorbance of radiation by intrinsic chromophores may be useful in determination of peptides/proteins, particularly at 280 nm ($A_{\lambda_{\max}} = 280$ nm), offering high specificity, arising strictly from tryptophan (W) and/or tyrosine (Y) residues (and from a small extent from disulphide bonds if present) [23]. On the other hand, optical properties of peptides/protein, containing no W and/or Y in their structure arising primarily from absorbance of peptide backbone and peptide bond [24]. UV/Vis spectrophotometry may be easily employed to obtain the basic information about amino acid composition.

3.3 Ion-exchange chromatography

As the next step, entire CD4 binding site was dissolved in ACS water in concentration of 1 mg.mL⁻¹ and directly analysed using ion-exchange chromatography (IEC) using Vis detection after ninhydrin derivatization to reveal the possible presence of undesired fragments occurred during synthesis (Fig. 2C). Although the most of peptide separations in the past 30 years have employed reverse-phase (RP) chromatography, in the past 10 years, cation exchange chromatography of peptides has developed into a significant complement to RP [25]. CD4 binding loop with pI calculated at 4.47 and net charge at 1.7 was identified at retention time of 75.12 minutes. Importantly, only very low amount of undesired fragments that belong to few unsuccessful steps in synthesis was determined, and recovery of peptide synthesis was therefore calculated up to 93.8 %. IEC was further employed for determination of amino acid composition of peptide after acidic hydrolysis using 6 M hydrochloric acid causing a destruction of the protein/peptide chain to amino acids that made up the initial molecule. As it can be seen in Fig. 2D, where entire chromatogram of IEC analysis is shown, all of amino acids (Asp; Ser; Glu; Gly; Pro; Met; Val; Ile; His) were determined in high amounts in their typical retention times. Hence, undesired fragments, observed using IEC analysis of whole peptide, are formed by amino acids used for CD4 binding site synthesis, not by other amino acids that may occur as the unwanted residues from previous syntheses or contamination. Therefore, synthesis process is not able to accomplish binding of all amino acid molecules used in synthesis and some of them form residual artefacts.

3.4 Matrix-assisted laser desorption/ionization time of flight mass spectrometry

Further, Matrix-assisted laser desorption/ionization time of flight mass spectrometry (MALDI-TOF MS) was utilized for characterization of CD4 binding site-like peptide synthesized by us (Fig. 2E). Peptide mass weight was calculated at 1098.13 Da. Using following analysis conditions: 2,5-dihydroxybenzoic acid (DHB) as the matrix, reflector positive mode with laser power of 70 %, signal at 1099.140 Da was observed and attributed to a quasimolecular ion $[M+H]^+$ formed from molecule of

peptide and proton resulted from charging through DHB matrix. Similarly, quasimolecular $[M+Na]^+$ with mass-to-charge ratio of 1121.166; and $[M+K]^+$ was also observed.

3.5 Influence of organic solvent on CD4 binding site electrochemical measurements

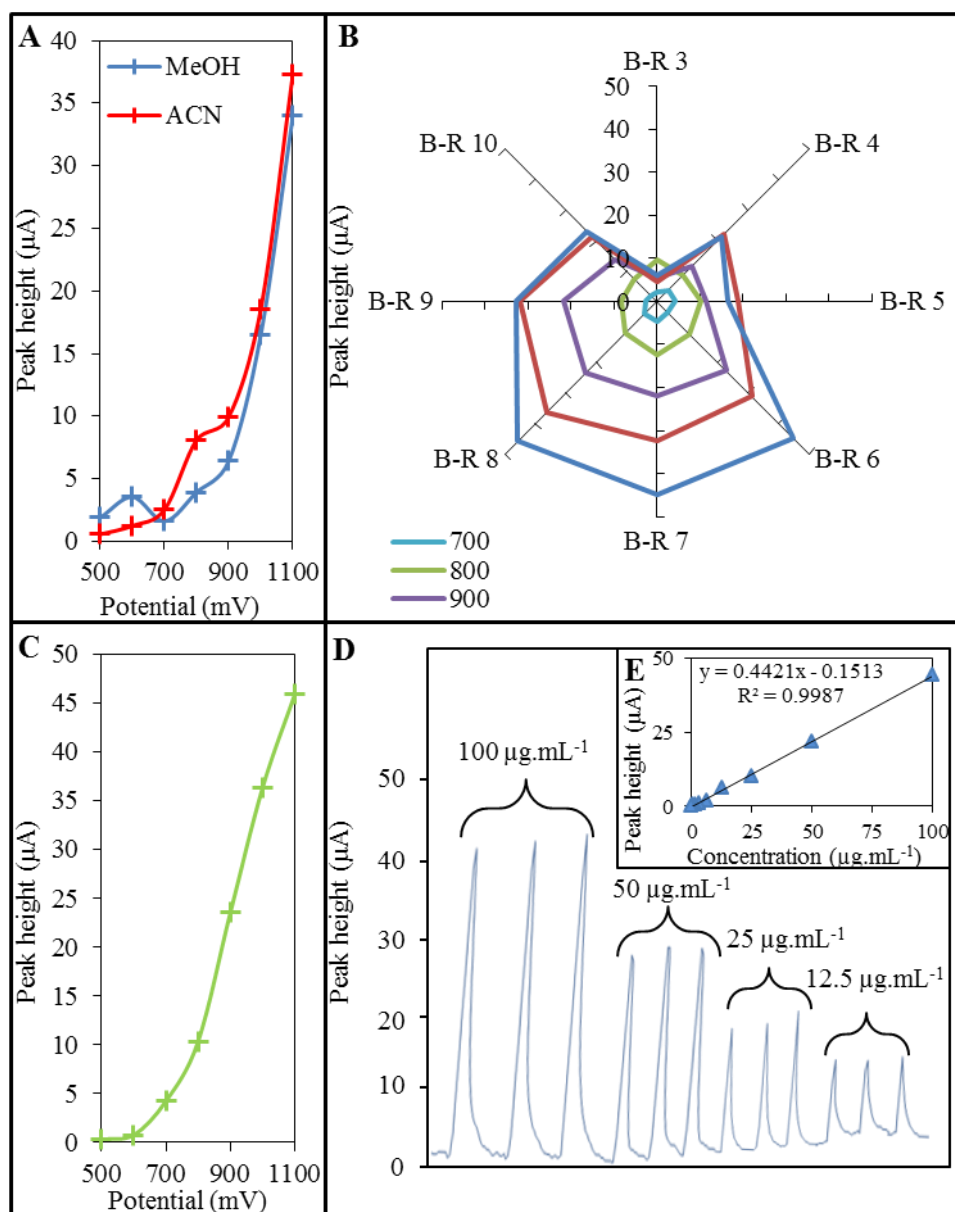


Figure 3. Optimization of Electrochemical detection of CD4 binding site of gp120 of HIV-1. Applied concentration of CD4 binding site-like peptide for analyses instead of calibration curves was $100 \mu g.mL^{-1}$. (A) Expression of influence of addition of organic solvents on amperometric signal of the peptide. MeOH – methanol, ACN – acetonitrile. (B) Optimization of potential for detection (500 – 1100 mV) of the peptide, and its behaviour under influence of Britton-Robinson buffer (pH 3 – 10). (C) Hydrodynamic voltammogram of CD4 binding site measured under optimized conditions (B-R pH 8, with 3% addition of CAN (v/v) in potential range 500 – 1100 mV). (D) Array record of CD4 binding site calibration curve measured within the range from 12.5 to $100 \mu g.mL^{-1}$. (E) Calibration curve measured within range from 12.5 to $100 \mu g.mL^{-1}$ using potential of 1100 mV.

After acquisition of basic spectroscopic characteristics, further we continued to the optimization of electrochemical detection of CD4 binding site of gp120. For electrochemical experiment, flow injection analysis (FIA) setup with electrochemical detector containing four analytical cells was employed.

Firstly, electrochemistry was utilized to monitor an effect of organic solvents in mobile phase on electrochemical response of peptide. As it can be seen in Fig. 3A, two organic solvents (MeOH – methanol, and ACN – acetonitrile) were tested in 3% addition into 80 mM trifluoroacetic acid (TFA) with pH 1.5 (*v/v*) used as a mobile phase. Analyses were performed within the potential range of 500 – 1100 mV, and it was shown that ACN supports the analysis at the ideal potential (1100 mV) more than MeOH (peak height of peptide for ACN 37.33 μA and for MeOH 33.99 μA). Therefore, 3% addition of acetonitrile to TFA (*v/v*) was chosen as beneficial to increase sensitivity in subsequent analyses.

3.6 Optimization of pH of mobile phase

Although TFA with 3% addition of ACN showed relatively good detector response of CD4 binding site-like peptide, we decided to test various pH buffers due to their ability to enhance the sensitivity of detection. Firstly, we tested various buffers as phosphate buffer, borate buffer, acetate buffer and Britton-Robinson (B-R) buffer, whereas B-R buffer was shown to have the greatest effect on peptide detection (data not shown). Hence, for further optimization experiments we utilized merely B-R buffer in pH range of 3 – 10 (3% addition of ACN (*v/v*)) and potentials within range between 700 – 1100 mV (Fig. 3B). As it is obvious from Fig. 3B, low pH maintained by B-R buffer with pH 3 was shown to influence the detection of peptide in sense of sensitivity. Ideal potential was determined at 800 mV showing peptide peak with height of 9.7 μA . After application of B-R buffer with pH 4 it was shown that ideal potential shifted to 1000 mV (peak height 21.8 μA) and the same phenomenon was observed at B-R buffer with pH 5 (peak height 16.5 μA). Interestingly, at pH 6 a significant change in electrochemical behaviour of CD4 binding site occurred. Ideal potential was determined at 1100 mV (peak height 44.7 μA) and the same trend was observed at all of B-R buffer pHs utilized (pH 7 – peak height 44.8 μA , pH 8 – peak height 45.9 μA). After application of B-R buffer, maintaining pH 9, rapid decrease of difference of peptide signal obtained when using detection potential 1000 mV (peak height 31.1 μA) and 1100 mV (peak height 32.7 μA) was observed. The same phenomenon was observed at B-R buffer of pH 10, where signal at 1100 mV was decreased to 6.0 μA (Fig. 3B). Based upon obtained data, it is obvious that B-R buffer with pH 8 shows the most beneficial effect on CD4 binding site detection, and therefore we decided to use it as mobile phase for subsequent analyses.

3.7 CD4 binding site-like peptide hydrodynamic voltammogram

Using the ideal conditions found from previous experiments (B-R buffer with pH 8, with 3% addition of ACN (*v/v*)) we carried out further analysis to obtain hydrodynamic voltammogram (HDV) of CD4 binding site. In ideal manner, the working electrode should be immersed to the supporting electrolyte and should give response only to the analysed substance in a thermodynamically defined,

potential-dependent fashion [26]. In our case hydrodynamic voltammetry was carried out within the potential range from 500 to 1100 mV (Fig. 3C). It clearly follows from the results obtained that the current response increases relatively slowly up to reaching interval of redox potential (800 mV). After reaching this “inflection point”, the current response increases rapidly to high oxidation potential, where maximal detection potential (1100 mV) was achieved as the ideal for peptide analyses (peak height 45.9 μA).

3.8 Analysis of CD4 binding site-like peptide in ideal conditions

After we optimized the electrochemical analysis of the peptide fragment, calibration curve was measured within the range from 12.5 to 100 $\mu\text{g.mL}^{-1}$. The array record obtained from calibration curve measurements is shown in Fig. 3D. From these data we constructed the calibration curve, which is shown in Fig. 3E. Under concentrations in above mentioned range, linear dependence of CD4 binding site-like peptide signal on its applied concentration ($y = 0.4421x - 0.1513$, $R^2 = 0.9987$) was obtained. Using the optimal conditions, we were able to estimate the detection limit (3 S/N) of the peptide as 0.04 $\mu\text{g.mL}^{-1}$. Other analytical parameters are shown in Tab. 1. Limit of quantification (10 S/N) was estimated as 0.1 $\mu\text{g.mL}^{-1}$.

Table 1. Parameters of electrochemical analysis of CD4 binding loop of gp120, where ¹ stays for molecular mass, ² for regression coefficient, ³ for limit of detection (3 S/N), ⁴ for limit of quantification (10 S/N) and ⁵ for relative standard deviation for injection of 20 μL .

Compound	Mr ¹	Regression equation	Linear dynamic range ($\mu\text{g.mL}^{-1}$)	R ²	LOD ³ ($\mu\text{g.mL}^{-1}$)	LOQ ⁴ ($\mu\text{g.mL}^{-1}$)	RSD (%)
CD binding loop	1098.13	$y = 0.4421x - 0.1513$	0.8 – 100.0	0.9987	0.04	0.1	2.2

4. CONCLUSION

In our study, we carried out the synthesis of peptide imitating the CD4 binding site by its amino acid sequence. Using spectroscopic methods we carried out basic characterization of substance, resulted from synthesis and moreover; we tested its purity that was established more than 90 %. For subsequent analyses, electrochemical measurement was employed to obtain information about the ideal conditions for CD4 binding site behaviour. Influence of organic solvent, type of buffer and influence of its pH on peptide current response were determined. Furthermore, the ideal detection potential was identified to provide complex information about CD4 binding site electrochemical properties. Optimized approach in this manner may serve as a tool for rapid and cheap method able to

determinate the peptide-peptide or protein-peptide interactions, which may be important for development of new therapeutic agents, able to block conservative CD4 binding site of gp120, and thus inhibit the ability of HIV-1 virions to form fusion with the host cells.

ACKNOWLEDGEMENTS

The authors acknowledge to NanoBioMetalNet CZ.1.07/2.4.00/31.0023 for financial support. Moreover, the authors wish to express their thanks to Lukas Melichar for perfect technical assistance.

CONFLICT OF INTEREST:

The authors have declared no conflict of interest.

References

1. J. Hemelaar, E. Gouws, P. D. Ghys and S. Osmanov, *Aids*, 25 (2011) 679.
2. D. L. Robertson, J. P. Anderson, J. A. Bradac, J. K. Carr, B. Foley, R. K. Funkhouser, F. Gao, B. H. Hahn, M. L. Kalish, C. Kuiken, G. H. Learn, T. Leitner, F. McCutchan, S. Osmanov, M. Peeters, D. Pieniazek, M. Salminen, P. M. Sharp, S. Wolinsky and B. Korber, *Science*, 288 (2000) 55.
3. D. A. Cooper, P. Maclean, R. Finlayson, H. M. Michelmore, J. Gold, B. Donovan, T. G. Barnes, P. Brooke and R. Penny, *Lancet*, 1 (1985) 537.
4. A. K. Rizos, I. Tsikalas, D. Morikis, P. Galanakis, G. A. Spyroulias and E. Krambovitis, *J. Non-Cryst. Solids*, 352 (2006) 4451.
5. R. Wyatt, P. D. Kwong, E. Desjardins, R. W. Sweet, J. Robinson, W. A. Hendrickson and J. G. Sodroski, *Nature*, 393 (1998) 705.
6. R. Wyatt and J. Sodroski, *Science*, 280 (1998) 1884.
7. B. S. Stein and E. G. Engleman, *J. Biol. Chem.*, 265 (1990) 2640.
8. R. L. Willey, J. S. Bonifacino, B. J. Potts, M. A. Martin and R. D. Klausner, *Proc. Natl. Acad. Sci. U. S. A.*, 85 (1988) 9580.
9. R. L. Dewar, M. B. Vasudevachari, V. Natarajan and N. P. Salzman, *J. Virol.*, 63 (1989) 2452.
10. E. Helseth, U. Olshevsky, C. Furman and J. Sodroski, *J. Virol.*, 65 (1991) 2119.
11. V. Sundaravaradan, S. R. Das, R. Ramakrishnan, S. Sehgal, S. Gopalan, N. Ahmad and S. Jameel, *Virology Journal*, 4 (2007).
12. I. Douagi, M. N. E. Forsell, C. Sundling, S. O'Dell, Y. Feng, P. Dosenovic, Y. X. Li, R. Seder, K. Lore, J. R. Mascola, R. T. Wyatt and G. B. K. Hedestam, *J. Virol.*, 84 (2010) 1683.
13. H. B. Bernstein, S. P. Tucker, S. R. Kar, S. A. McPherson, D. T. McPherson, J. W. Dubay, J. Lebowitz, R. W. Compans and E. Hunter, *J. Virol.*, 69 (1995) 2745.
14. A. Zafiroopoulos, S. Baritaki, Z. Vlata, D. A. Spandidos and E. Krambovitis, *Biochem. Biophys. Res. Commun.*, 284 (2001) 875.
15. W. Weissenhorn, A. Dessen, S. C. Harrison, J. J. Skehel and D. C. Wiley, *Nature*, 387 (1997) 426.
16. C. T. Wild, D. C. Shugars, T. K. Greenwell, C. B. McDanal and T. J. Matthews, *Proc. Natl. Acad. Sci. U. S. A.*, 91 (1994) 9770.
17. M. Lu, S. C. Blacklow and P. S. Kim, *Nat. Struct. Biol.*, 2 (1995) 1075.
18. O. Zitka, N. Cernei, Z. Heger, M. Matousek, P. Kopel, J. Kynicky, M. Masarik, R. Kizek and V. Adam, *Electrophoresis*, 34 (2013) 2639.
19. G. L. Long and J. D. Winefordner, *Anal. Chem.*, 55 (1983) 712.
20. M. D. Hazenberg, D. Hamann, H. Schuitemaker and F. Miedema, *Nat. Immunol.*, 1 (2000) 285.
21. J. B. Alimonti, T. B. Ball and K. R. Fowke, *J. Gen. Virol.*, 84 (2003) 1649.

22. G. B. Fields and R. L. Noble, *Int. J. Pept. Protein Res.*, 35 (1990) 161.
23. C. N. Pace, F. Vajdos, L. Fee, G. Grimsley and T. Gray, *Protein Sci.*, 4 (1995) 2411.
24. N. J. Anthis and G. M. Clore, *Protein Sci.*, 22 (2013) 851.
25. A. J. Alpert, K. Petritis, L. Kangas, R. D. Smith, K. Mechtler, G. Mitulovic, S. Mohammed and A. J. R. Heck, *Anal. Chem.*, 82 (2010) 5253.
26. O. Zitka, M. Kominkova, S. Skalickova, H. Skutkova, I. Provaznik, T. Eckschlager, M. Stiborova, V. Adam, L. Trnkova and R. Kizek, *Int. J. Electrochem. Sci.*, 7 (2012) 10544.

© 2014 The Authors. Published by ESG (www.electrochemsci.org). This article is an open access article distributed under the terms and conditions of the Creative Commons Attribution license (<http://creativecommons.org/licenses/by/4.0/>).